Structural Characterization of the Active Site of Brucella abortus Cu-Zn Superoxide Dismutase: A 15N and 1H NMR Investigation

ARTICLE *in* BIOCHEMISTRY · OCTOBER 1995

Impact Factor: 3.02 · DOI: 10.1021/bi00038a022 · Source: PubMed

5 AUTHORS, INCLUDING:

Robert W Thornburg
Iowa State University
74 PUBLICATIONS **2,467** CITATIONS

SEE PROFILE

Louisa Tabatabai
Iowa State University
82 PUBLICATIONS **1,388** CITATIONS

SEE PROFILE

Structural Characterization of the Active Site of *Brucella abortus* Cu−Zn Superoxide Dismutase: A ^{15}N and ^{1}H NMR Investigation†

Yen-Liang Chen, Sanggyu Park, Robert W. Thornburg, Louisa B. Tabatabai,‡ and Agustin Kintanar*

Department of Biochemistry and Biophysics, Iowa State University, Ames, Iowa 50011

Received March 22, 1995; Revised Manuscript Received July 5, 1995®

ABSTRACT: Prokaryotic Cu−Zn superoxide dismutases (SODs) are rare and poorly characterized compared to their eukaryotic counterparts. To better characterize the structure of the prokaryotic enzyme, an NMR investigation of *Brucella abortus* Cu−Zn SOD in the reduced form was undertaken. The enzyme studied was a recombinant form, expressed in *Escherichia coli*. The enzyme initially lacked a full complement of Cu and Zn ion. After demetallation and remetallation with a stoichiometric amount of Cu and Zn ion, the specific activity of the recombinant *B. abortus* Cu−Zn SOD was comparable to the specific activity of the bovine enzyme. The ^{15}N and ^{1}H resonances of seven active site histidine imidazole rings were assigned using two-dimensional NMR methods. A self-consistent set of nuclear Overhauser effects between imidazole ring protons was observed, which was in agreement with the predictions of a model based on the X-ray crystallographic structure of the oxidized bovine enzyme (Tainer, J. A., Getzoff, E. D., Beem, K. M., Richardson, J. S., & Richardson, D. C. (1982) *J. Mol. Biol. 160*, 181−217). These observations strongly suggest that the structure of the active site of the prokaryotic enzyme is similar to that of the eukaryotic enzyme. Differences in the observed and predicted nuclear Overhauser effects could be ascribed to differences in the oxidation state of the Cu ion (Cu(I) in the reduced *B. abortus* enzyme and Cu(II) in the oxidized bovine enzyme), as much as they could to the different origins of the enzymes. The NMR data were also compared to a similar ^{1}H NMR study of the human enzyme (Bertini, I., Capozzi, F., Luchinat, C., Piccioli, M., & Viezzoli, M. S. (1991) *Eur. J. Biochem. 197*, 691−697). The pattern of nuclear Overhauser effects and the chemical shifts of corresponding resonances were very similar in ^{1}H NMR spectra of the human and *B. abortus* enzymes. Significant differences in the chemical shifts or exchange behavior of a few resonances indicated differences in the environments of several histidines in the active sites of reduced *B. abortus* and human Cu−Zn SODs. This is consistent with the presence of a number of insertions and deletions in the loop regions that make up the active site as indicated by amino acid sequence alignment studies. The tautomeric and protonation states of the active site histidines were also determined in this study, and the results were in agreement with previous studies. The resonances of nitrogen atoms coordinated to metal ions were found to fall between those of protonated and unprotonated nitrogens on histidine imidazoles.

Superoxide dismutase (SOD)[1] enzymes protect cells against the cytotoxic activity of the superoxide radical ($O_2^{\bullet-}$), which is a byproduct of aerobic metabolism (Fridovich, 1986; Bannister *et al.*, 1987). One class of these enzymes, the copper−zinc SODs, occurs primarily in the cytoplasm of eukaryotes. The eukaryotic Cu−Zn SODs have been studied in some detail. The enzyme is a homodimer of ~32 kDa. Each subunit comprises ~153 amino acids and binds one Cu and one Zn ion. The dismutation of $O_2^{\bullet-}$ proceeds via alternate reduction and oxidation of the essential Cu ion during successive encounters with the substrate to produce O_2 and H_2O_2, respectively (Fridovich, 1986). Both steps occur with a rate constant of 2×10^9 M^{-1} s^{-1} (Klug *et al.*, 1972; Rotilio *et al.*, 1972; Fee & Bull, 1986) which approaches the diffusion-controlled limit. The subunit association in eukaryotic Cu-Zn SODs is very tight, and the enzyme is very stable. Cu−Zn SOD from bovine erythrocytes remains active even in 8 M urea (Forman & Fridovich, 1973; Malinowski & Fridovich, 1979) and 4% sodium dodecyl sulfate (Forman & Fridovich, 1973) and remains folded above 90 °C (Roe *et al.*, 1988). The enzyme can be demetallated and reconstituted with other metal ions besides Cu and Zn (Beem *et al.*, 1974; Valentine *et al.*, 1979). The presence of bound metals greatly increases the thermal stability of the enzyme (Forman & Fridovich, 1973; Roe *et al.*, 1988).

High resolution crystal structures of the oxidized form of bovine enzyme (Tainer *et al.*, 1982) and the recombinant human enzyme (Parge *et al.*, 1992) have been determined. The active site has four conserved histidines coordinated to the Cu^{2+} ion. One of these histidines is also a bridging ligand with the Zn^{2+} ion. Two additional histidines and an aspartate residue are also coordinated to the Zn^{2+} ion. A seventh histidine is buried near the active site, is positively charged

† Support for this investigation was provided by Iowa Agriculture and Home Economics Experiment Station, Project No. 3058.

* To whom correspondence should be addressed.

‡ National Animal Disease Center, U.S. Department of Agriculture, Ames, IA 50010.

® Abstract published in *Advance ACS Abstracts,* September 1, 1995.

[1] Abbreviations: EDTA, ethylenediaminetetraacetic acid; HMQC, two-dimensional heteronuclear multiple quantum coherence spectroscopy; IPTG, isopropyl β-D-thiogalactopyranoside; NOE, nuclear Overhauser effect; NOESY, two-dimensional nuclear Overhauser enhancement spectroscopy; PAGE, polyacrylamide gel electrophoresis; PCR, polymerase chain reaction; SDS, sodium dodecyl sulfate; SOD, superoxide dismutase; TPPI, time proportional phase incrementation.

0006-2960/95/0434-12265$09.00/0

even at high pH, and is hydrogen-bonded to two main-chain carbonyl oxygen atoms, one of which belongs to a Cu histidine ligand.

Eukaryotic Cu−Zn SODs have also been studied by ^{1}H NMR spectroscopy, with most of the attention focused on the resonances of exchangeable and nonexchangeable protons of histidine imidazole rings (Cass *et al.*, 1977, 1979; Lippard *et al.*, 1977; Stoesz *et al.*, 1979; Burger *et al.*, 1980; Paci *et al.*, 1990; Bertini *et al.*, 1991). These studies reveal the following: a conformational change in the apoenzyme upon binding of Zn (Lipard *et al.*, 1977; Cass *et al.*, 1979); a protonated histidine imidazole with a pK_a over 9 that is not a metal ligand (Cass *et al.*, 1977; Stoesz *et al.*, 1979); and from NOE data, a similar active site structure of reduced eukaryotic Cu−Zn SODs (Stoesz *et al.*, 1979; Burger *et al.*, 1980; Paci *et al.*, 1990; Bertini *et al.*, 1991) and oxidized eukaryotic Cu−Zn SODs (Tainer *et al.*, 1982; Parge *et al.*, 1992).

For many years, only one example of a prokaryotic Cu−Zn SOD was known (Puget & Michelson, 1974), from *Photobacterium leiognathi*, a luminescent bacterium and symbiont of ponyfish. Since then, a number of other prokaryotic Cu−Zn SODs have been found in *Caulobacter crescentus* (Steinman, 1982), *Pseudomonas maltophilia* and *Pseudomonas diminuta* (Steinman, 1985), *Brucella abortus* (Beck *et al.*, 1990), and *Haemophilus* species (Kroll *et al.*, 1991). There is evidence that prokaryotic Cu−Zn SODs are secreted (Steinman, 1987; Steinman & Ely, 1990; Beck *et al.*, 1990; Bricker *et al.*, 1990; Kroll *et al.*, 1991), suggesting that the bacterial enzyme is involved in dismutation of extracellular $O_2^{\bullet-}$.

The primary sequences of five bacterial Cu−Zn SODs are known: two from *Haemophilus* species (Kroll *et al.*, 1991), from *B. abortus* (Beck *et al.*, 1990), from *C. crescentus* (Steinman & Ely, 1990), and from *P. leiognathi* (Steffens *et al.*, 1983). The functionally and structurally important amino acids in eukaryotic Cu−Zn SODs are well-known from sequence alignment (Getzoff *et al.*, 1989) and from numerous studies of the structure and function of these enzymes. Sequence alignment of the prokaryotic Cu−Zn SODs reveals a strong conservation of these functionally and structurally important amino acid residues (Getzoff *et al.*, 1989; Steinman & Ely, 1990; Kroll *et al.*, 1991), suggesting that the polypeptide fold of Cu−Zn SOD is also conserved among prokaryotes and eukaryotes (Steinman & Ely, 1990). A number of gaps and insertions are required to align the Cu−Zn SOD sequences of prokaryotes with those of eukaryotes, and these occur primarily in loop regions that make up the active site (Getzoff *et al.*, 1989; Steinman & Ely, 1990).

Structural and functional characterizations of prokaryotic Cu−Zn SODs have been few. The *Photobacterium* and *Caulobacter* enzymes are both homodimers with the expected molecular mass of ~32 kDa (Martin & Fridovich, 1981; Steinman, 1982). Both the *Photobacterium* and *Caulobacter* enzymes bind near-stoichiometric amounts of Cu and Zn (Steinman, 1982; Puget *et al.*, 1977), have basic p*I* values around 8 (Steinman, 1982; Martin & Fridovich, 1981), and have specific activities in the range of other Cu-Zn SODs (Steinman, 1982; Martin & Fridovich, 1981). A preliminary crystallographic characterization of the *Photobacterium* Cu−Zn SOD has been reported (Redford *et al.*, 1990), but a high resolution structure has not yet been published. Further investigations of the structure and function of prokaryotic Cu−Zn SODs are therefore required to answer some pertinent questions. Are the structures of the active sites of the prokaryotic and eukaryotic enzymes similar? How are the gaps and insertions in the prokaryotic sequence accommodated in the polypeptide fold? Is the subunit association in the prokaryotic enzyme as strong as in the eukaryotic enzyme? Are differences in the characteristics of the prokaryotic and eukaryotic enzymes relevant to the periplasmic location of the former? These are just a few of the questions that come to mind.

In this paper, we characterize the structure and function of Cu−Zn SOD from *B. abortus* by atomic absorption spectroscopy, SOD activity assay, and ^{1}H and ^{15}N NMR spectroscopy. The *B. abortus* Cu−Zn SOD studied here was expressed in *Escherichia coli*. Previous studies showed that the recombinant and native *B. abortus* Cu−Zn SODs were identical by the criteria of SDS−PAGE, N-terminal amino acid sequencing, and immunologic cross-reactivity (Bricker *et al.*, 1990). We report the systematic assignment of the ^{15}N and exchangeable and nonexchangeable proton NMR resonances of histidine imidazole rings in the active site of reduced *B. abortus* Cu−Zn SOD. The chemical shift and NOE data indicate a strong similarity of the structure of the active site of prokaryotic and eukaryotic Cu−Zn SODs in the reduced form.

MATERIALS AND METHODS

Efficient Expression of Cu−Zn SOD. The plasmid containing the full-length *B. abortus* Cu−Zn SOD gene (pBA20-1527; Bricker *et al.*, 1990) was purified by standard methods (Sambrook *et al.*, 1989). A pair of restriction enzyme sites (*Xba*I at the 5′ end and *Bgl*II at the 3′ end) were incorporated into the desired sequence by PCR amplification (Saiki *et al.*, 1988) using the oligonucleotide primers 5′-GCGGTTTCT-CTAGAACTGTTCTAAC-3′ and 5′-GGGGAATCAGATCT-CAAGAATTGGG-3′. These PCR primers were designed to hybridize to the *B. abortus* Cu−Zn SOD gene (Chin, Tabatabai, and Mayfield, unpublished results) at sites downstream and upstream of the coding region. The oligonucleotides were synthesized by the Nucleic Acids Facility at Iowa State University using standard solid-phase methods. The PCR amplification was performed with a PCR kit from Perkin-Elmer Cetus. The 598 bp PCR-amplified fragment was purified by electrophoresis on 2% agarose gels, and the band having the desired length was electroeluted from the gel (Sambrook *et al.*, 1989). Following cleanup by phenol, chloroform, and ethanol precipitation, the fragment was digested with *Xba*I and *Bgl*II, mixed with *Xba*I/*Bam*HI-digested pET3c (Rosenberg *et al.*, 1987), ligated, and transformed into *E. coli* strain TG1. All digestions, ligations, transformations, and other manipulations were performed by standard protocols (Sambrook *et al.*, 1989).

Plasmids were screened for the presence of the inserted fragment. Several plasmids with the correct sized insert were selected for sequencing. Automated DNA sequencing was performed by the Nucleic Acids Facility at Iowa State University. The insert from one plasmid, pBASOD-1, was completely sequenced. DNA sequence analysis showed that the *B. abortus* Cu−Zn SOD gene coding for the mature protein and a leader sequence directing secretion into the periplasm (Chin, Tabatabai, and Mayfield, unpublished results) was incorporated in the plasmid. There were two nucleotide substitutions in the coding region relative to the

previously determined DNA sequence of the *B. abortus* Cu−Zn SOD gene (Chin, Tabatabai, and Mayfield, unpublished results); but one mutation was silent, coding for the same amino acid, and the other mutation resulted in a conservative change of valine to alanine in the peptide leader. The pBASOD-1 plasmid was isolated and used to transform *E. coli* BL21(DE3) (Studier & Moffat, 1986). This lysogen carries the T7 polymerase gene under the control of the Lac UV5 promoter. The pBASOD-1 plasmid, a derivative of pET3c, contains the *B. abortus* Cu−Zn SOD gene under the control of the strong bacteriophage T7 promoter. Thus, *E. coli* BL21(DE3) transformed with pBASOD-1 produces recombinant *B. abortus* Cu−Zn SOD with IPTG induction.

Purification of Recombinant Cu−Zn SOD. Strains used for overproduction of *B. abortus* Cu−Zn SOD were *E. coli* 71/18 containing pBA20-1527 (Bricker *et al.*, 1990) and *E. coli* BL21(DE3) containing pBASOD-1. The strains were grown in either LB or minimal M9 medium supplemented with vitamins and nucleotides (Hoffman & Spicer, 1991). IPTG was typically added when the culture reached an optical density (A_{600}) of 1.5, and the culture was maintained for at least 4 h after induction, before harvest. Separate cell culture experiments indicated that these conditions gave the optimum protein yield (Chen and Kintanar, unpublished results). For production of uniformly ^{15}N-labeled enzyme, the same supplemented minimal M9 medium was used, except ^{15}N-labeled ammonium chloride (1 g/L of culture) was substituted as the nitrogen source.

The recombinant protein was purified basically by the procedure described in Bricker *et al.* (1990). The cells were pelleted by centrifugation at 3000*g* for 15 min, and Cu−Zn SOD was extracted from the periplasm by resuspension in 2 mL of extraction buffer (10 mM sodium phosphate, 0.1% Triton X-100, pH 7.5)/g of packed cells. The suspension was shaken overnight at 37 °C, and the cells were again pelleted by centrifugation. The supernatant was decanted and saved, and the pellets were washed by resuspension in a small volume of extraction buffer and subsequent centrifugation. The combined supernatants were then dialyzed extensively against several changes of low salt buffer (10 mM sodium phosphate, 5 mM sodium chloride, pH 6.4). After removal of a nonproteinaceous precipitate by centrifugation, the clarified dialysate was loaded onto a 2.5 cm × 60 cm Fast Flow CM-Sepharose column (Pharmacia, Inc.) equilibrated with low salt buffer. The column was washed with 2−3 volumes of low salt buffer and eluted with a 5−600 mM linear sodium chloride gradient (600 mL of total volume). The elution profile was monitored by UV spectroscopy at 230 nm, and the main elution peak containing the SOD was further analyzed by SDS−PAGE using the method of Laemmli (1970) and visualized by Coomassie Blue R-250 staining. Fractions containing SOD were pooled, dialyzed against the low salt buffer, and lyophilized.

The activity of Cu−Zn SOD was determined by the method of McCord and Fridovich (1969), which measures the inhibition of the reduction of cytochrome *c* by xanthine oxidase-generated $O_2^{\bullet-}$. All materials used in the assay were purchased from Sigma, including Cu−Zn SOD from bovine erythrocytes used as a control. Protein concentrations were determined using the Folin Lowry method (Lowry *et al.*, 1951) with bovine erythrocyte Cu−Zn SOD as the standard. All reagents for the protein concentration assay were obtained from Sigma.

Sample Preparation. The recombinant *B. abortus* Cu−Zn SOD was demetallated and reconstituted with Cu^{2+} and Zn^{2+} by the method of Beem *et al.* (1974). Protein solutions were transferred into a low pH acetate buffer (10 mM sodium acetate, pH 3.8) by dialysis and run on a Sephadex G-25 (Pharmacia) gel filtration column equilibrated with 10 mM EDTA and the low pH acetate buffer. Fractions containing protein were pooled and dialyzed against the acetate buffer to remove most of the EDTA and then run on a Sephadex G-25 gel filtration column equilibrated with 10 mM magnesium chloride and the acetate buffer to remove residual EDTA. Fractions containing protein were pooled and lyophilized, dissolved in water, and dialyzed against the acetate buffer to remove Mg^{2+}. The apoenzyme was adjusted to a concentration of 1 mg/mL, and a stoichiometric amount (10% excess) of a 200 μg/mL copper sulfate solution was slowly added. The resulting solution was stirred, allowed to equilibrate overnight at 4 °C, and then dialyzed against 50 mM sodium phosphate buffer at pH 6. The protein was then infused with zinc by addition of a stoichiometric amount (10% excess) of zinc chloride (200 μg/mL), followed by stirring and equilibration at 4 °C overnight. Finally, the remetallated Cu−Zn SOD was dialyzed against low salt buffer.

For NMR samples, the protein solution in low salt buffer was concentrated by centrifugal filtration over a 10-kDa cutoff membrane. Typical NMR samples contained 25−35 mg of the recombinant protein. The concentrated protein solution (~350 μL) was transferred into a Wilmad 528pp NMR tube. Just prior to NMR spectroscopy, a 1.5 molar excess of sodium dithionite (freshly prepared, concentrated aqueous solution) was added to reduce Cu^{2+} and 45 μL of D_2O was added to provide a lock signal. The final sample volume was adjusted to 450 μL with the low salt buffer. All NMR spectra shown here were obtained on remetallated and reduced *B. abortus* Cu−Zn SOD.

NMR Spectroscopy. All NMR spectroscopy was performed on a Varian Instruments UNITY-500 NMR spectrometer at a ^1H resonance frequency of 499.843 MHz and a ^{15}N resonance frequency of 50.653 MHz. All ^1H NMR spectra were referenced to the H_2O peak, which was assumed to resonate at 4.80 ppm at 22 °C and shift upfield 5 Hz/°C with increasing temperature. The ^{15}N spectra were referenced to external $^{15}NH_4Cl$ (2.9 M) in 1 M HCl at 20 °C, which was assumed to resonate at 24.93 ppm relative to the NH_3 resonance (Levy & Lichter, 1979). The ^{15}N chemical shifts were not corrected for temperature. The temperature of the NMR sample was regulated by heated (or cooled) air flow and was measured by thermocouple near the sample coil. The temperatures were accurate to ±0.5 °C.

One-dimensional NMR spectra were collected with the H_2O resonance suppressed using the 1-1 spin-echo selective excitation pulse sequence (Sklenar & Bax, 1987). Typical parameter settings and data processing were as described previously (Kintanar *et al.*, 1991). One-dimensional NOE experiments were performed with a pulse sequence consisting of a 100 ms presaturation pulse followed by a jump-return pulse (Plateau & Guéron, 1982) to suppress the H_2O resonance. The presaturation pulse was of sufficient power to saturate the irradiated peak by ~90%. The NOE data were obtained by taking the difference between the spectrum collected with the presaturation pulse centered on the peak of interest and a control spectrum collected with the

presaturation pulse set off-resonance, well downfield. Typically, 1600 scans were collected at each frequency offset. The delay between the pulses of the jump-return sequence was typically 40 μs to allow good excitation of the downfield imino resonances. Other spectral and data processing parameters were similar to those for the 1-1 echo one-dimensional ^{1}H NMR experiments.

The two-dimensional NOESY spectrum (Jeener *et al.*, 1979) was acquired using the method of States *et al.* (1982) to achieve phase sensitive detection in the first dimension. There were 2048 complex points acquired in the t_2 dimension, and 300 hypercomplex pairs were acquired in the t_1 dimension. The sweep width was set to 12 000 Hz in both dimensions. The mixing time was 150 ms, and 64 scans were collected per t_1 point. The 90° pulse was 9 μs, and the recycle delay was 1.8 s. The H_2O resonance was suppressed by presaturation for 1 s during the recycle delay just prior to the first NOESY pulse.

A two-dimensional ^{15}N−^{1}H HMQC spectrum (Bax *et al.*, 1983; Summers *et al.*, 1986) was acquired using TPPI (Drobny *et al.*, 1979; Marion & Wüthrich, 1983) to achieve phase sensitive detection in the first (^{15}N) dimension. Typically, 2048 complex t_2 points and 256 t_1 increments were acquired. The sweepwidth was 8000 or 12 000 Hz in the ^{1}H dimension and 4000 Hz in the ^{15}N dimension. The delay during which the ^{15}N and ^{1}H signals become antiphase (Δ) was set at 25 ms, to optimize a heteronuclear J coupling of 20 Hz, and 64 scans were collected per t_1 point. The ^{1}H 90° pulse was 13 μs, the ^{15}N 90° pulse was 60 μs, and the recycle delay was 1.8 s. The residual H_2O resonance was suppressed by very low power presaturation for 1 s just prior to the first ^{1}H HMQC pulse. During acquisition, ^{15}N was decoupled using a WALTZ pulse sequence (Shaka *et al.*, 1983) and a 1.25 kHz decoupling field.

Two-dimensional spectra were processed with either Varian software or Felix 2.05 (Hare Research Inc.). The data were zero-filled to 1024 points in the t_1 dimension and were apodized with 60° shifted sine bell filters in both dimensions.

RESULTS

Expression, Purification, and Remetallation of Recombinant Cu−Zn SOD. The strain *E. coli* 71/18 containing the original plasmid pBA20-1527 (Bricker *et al.*, 1990) yielded 12 mg of purified Cu−Zn SOD/L of culture in LB. When this strain was grown in the minimal medium, the yield dropped to 1 mg/L of culture. This yield is too low for cost-effective incorporation of stable isotopes into the protein. Therefore, the gene for *B. abortus* Cu−Zn SOD was transferred into a more efficient expression system based on T7 RNA polymerase (Studier & Moffat, 1986) by constructing the vector pBASOD-1. The *E. coli* BL21(DE3) lysogen containing the pBASOD-1 plasmid yielded 20 mg of purified Cu−Zn SOD/L of culture in supplemented minimal medium. This overproducing strain was used for subsequent production of recombinant *B. abortus* Cu−Zn SOD.

The *B. abortus* Cu−Zn SOD is a periplasmic protein (Beck *et al.*, 1990; Bricker *et al.*, 1990). The cloned gene codes for a preprotein with a peptide leader sequence which directs secretion of the protein and is subsequently cleaved to give the mature protein (Chin, Tabatabai, and Mayfield, unpublished results). The N-terminal sequences of Cu−Zn SOD expressed in *E. coli* and of the native protein purified from *B. abortus* are identical (Bricker *et al.*, 1990), indicating that the recombinant Cu−Zn SOD is properly processed during secretion in *E. coli*. It is assumed that the recombinant enzyme expressed from pBASOD-1 in *E. coli* BL21(DE3) is also properly secreted and processed. This is supported by the fact that the purification protocol, which was designed for a periplasmic protein, still works. Furthermore, *B. abortus* Cu−Zn SOD expressed from pBA20-1527 or pBASOD-1 could not be distinguished by SDS−PAGE, gel filtration chromatography, or ^{1}H NMR spectroscopy (data not shown).

The purified recombinant Cu−Zn SOD had a low specific activity, typically less than 200 units/mg, more than an order of magnitude less than the previously reported specific activity of the bovine enzyme (McCord & Fridovich, 1969). A concentrated solution of the purified *B. abortus* protein appeared clear and not the blue-green seen with concentrated solutions of eukaryotic Cu−Zn SOD, suggesting that the recombinant *B. abortus* Cu−Zn SOD did not have the full complement of metal ions. Metal analysis by atomic absorption spectroscopy indicated less than 0.05 equiv of Cu or Zn ion per subunit of enzyme. After demetallation and reconstitution with stoichiometric amounts of Cu and Zn ion, the *B. abortus* Cu−Zn SOD had a specific activity of 3800 units/mg, comparable to the 3400 units/mg of protein reported for the bovine enzyme (McCord & Fridovich, 1969). Metal analysis showed that the remetallated enzyme had a full complement of Cu ion and at least 0.9 equiv of Zn ion per subunit. The apoenzyme was found to be unstable over a period of a few days and was therefore remetallated as soon as possible after demetallation.

The absence of a full complement of Cu and Zn ion in the recombinant enzyme was not an artifact of the purification procedure. This was verified by subjecting a remetallated protein sample to the entire protocol. Metal analysis, activity assay, and ^{1}H NMR spectroscopy indicated that no metal was lost during the procedure (data not shown). In the native protein isolated from cultures of *B. abortus*, metal analysis indicates greater than 0.4 equiv of Cu and 0.8 equiv of Zn per subunit, and the specific activity of the enzyme is comparable to that of bovine Cu−Zn SOD and remetallated, recombinant *B. abortus* Cu−Zn SOD.

NMR Spectroscopy of the Recombinant Cu−Zn SOD. The downfield regions of the ^{1}H NMR spectra of unlabeled and ^{15}N-labeled recombinant *B. abortus* Cu−Zn SOD are shown in Figure 1. The region of the spectrum downfield of 10 ppm is expected to contain resonances arising from nitrogen-bound protons of histidine imidazole rings, tryptophan indole rings, and peptide amides (Robillard & Shulman, 1974; Stoesz *et al.*, 1979; Wüthrich, 1986). The *B. abortus* Cu−Zn SOD contains no tryptophan residues (Beck *et al.*, 1990). The spectra of the unlabeled and ^{15}N-labeled protein are very similar. The main difference is the presence of a 90 Hz splitting in the peaks of the ^{15}N-labeled protein spectrum (Figure 1b). This splitting is due to a ^{15}N−^{1}H one-bond scalar coupling and confirms that the downfield resonances arise from protons bound to nitrogen. Seven resonances are labeled in the ^{1}H spectra of Cu−Zn SOD. These resonances arise from imidazole protons, and they are labeled in a manner to permit easy comparison with previous ^{1}H NMR resonance assignments of eukaryotic Cu−Zn SODs (Stoesz *et al.*, 1979; Bertini *et al.*, 1991).

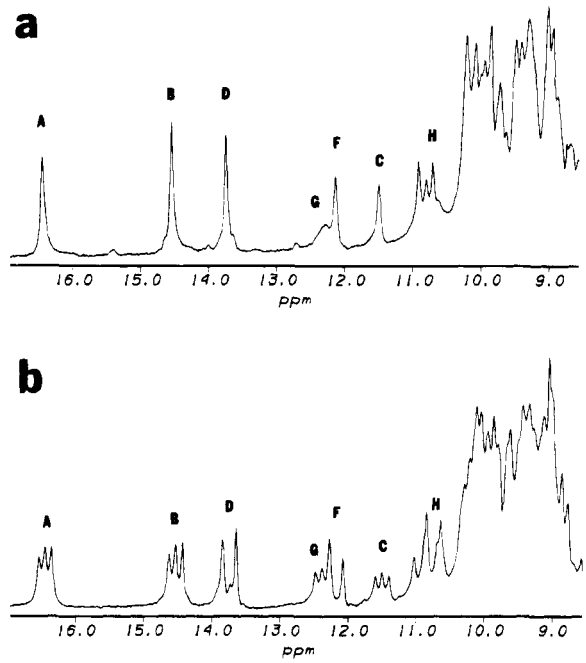

FIGURE 1: Downfield region of the ^1H NMR spectra of *B. abortus* Cu−Zn SOD showing the exchangeable proton resonances of active site histidine residues. The spectra were recorded at 30 °C. Solution conditions were as described in the text. The H_2O resonance was suppressed using the 1-1 echo pulse sequence. (a) Unlabeled protein. (b) Uniformly ^{15}N-labeled protein.

An interesting feature of the ^1H NMR spectrum of the ^{15}N-labeled *B. abortus* Cu−Zn SOD is the presence of residual unsplit peaks at some positions, e.g., peaks A, B, C, and G (Figure 1b). This results from isotopic dilution of the ^{15}N label by ^{14}N coming from the unlabeled nucleotides or vitamins in the culture medium. The most probable isotopic dilution would occur during histidine biosynthesis from ATP, which would result in the misincorporation of ^{14}N at Nϵ2 of the imidazole ring (Zubay, 1988). Thus, peaks A, B, C, and G probably arise from Nϵ2 protons of histidine imidazole rings. There is no evidence of significant isotopic dilution of backbone or side-chain amide nitrogens, or of Nδ1 on histidine imidazole rings (Chen and Kintanar, unpublished results).

Imidazole Tautomeric States and Resonance Connectivity from Coherence Transfer Spectroscopy. Resonances arising from histidines are readily verified by the two-dimensional $^{15}N-^1H$ HMQC spectrum. The nitrogen atoms in an imidazole ring may be classified as one of three types ($\alpha+$, α, and β), each with a characteristic chemical shift (Witanowski *et al.*, 1972; Blomberg *et al.*, 1977; Bachovkin & Roberts, 1978; Harbison *et al.*, 1981; Munowitz *et al.*, 1982; Roberts *et al.*, 1982; Bachovkin, 1986). The $\alpha+$ nitrogen is found in positively charged imidazole rings and has a characteristic chemical shift of 176.5 ppm relative to external liquid NH_3 (Bachovkin, 1986; Pelton *et al.*, 1993). The α nitrogen is protonated and on a neutral imidazole ring, and it has a characteristic chemical shift of 167.5 ppm; while the β nitrogen is unprotonated and on a neutral imidazole ring, and it resonates at 249.5 ppm (Bachovkin, 1986; Pelton *et al.*, 1993). In the proper region of the $^{15}N-^1H$ HMQC spectrum, there appear cross-peaks correlating the nitrogens with the nonexchangeable protons in a histidine imidazole ring, and the pattern of cross-peaks can indicate the tautomeric form of the histidine residue (van Dijk *et al.*, 1992; Pelton *et al.*, 1993). In particular, the Nϵ2−H tautomer should show a single strong Nδ1−Hϵ1 cross-peak at a ^{15}N chemical shift around 250 ppm and a pair of weaker Nϵ2−Hϵ1 and Nϵ2−Hδ2 cross-peaks at a ^{15}N chemical shift around 168 ppm (Pelton *et al.*, 1993). In contrast, the Nδ1−H tautomer should show a pair of strong Nϵ2−Hϵ1 and Nϵ2−Hδ2 cross-peaks at a ^{15}N chemical shift around 250 ppm and a pair of weaker Nδ1−Hϵ1 and Nδ1−Hδ2 cross-peaks at a ^{15}N chemical shift around 168 ppm (Pelton *et al.*, 1993). Finally, a positively charged histidine imidazole should show two pairs of cross-peaks with similar ^{15}N chemical shifts around 177 ppm (Pelton *et al.*, 1993).

The appropriate spectral region of the $^{15}N-^1H$ HMQC spectrum of ^{15}N-labeled recombinant *B. abortus* Cu−Zn SOD is shown in Figure 2a. The numbers on the cross-peaks index the resonances of nonexchangeable imidazole protons. These resonances are labeled in a manner to permit easy comparison with previous ^1H NMR resonance assignments of nonexchangeable imidazole protons in human Cu−Zn SODs (Bertini *et al.*, 1991). Cross-peaks belonging to the same imidazole ring are joined by lines. Seven spin systems of a possible 11 are observed. The remaining four histidine spin systems are presumably not observed because of broadening of the resonances by chemical exchange.

A slightly different expansion of the same HMQC spectrum is shown in Figure 2b. Cross-peaks between the downfield exchangeable imidazole protons and type α and $\alpha+$ imidazole nitrogens are observed, allowing further correlation of imidazole spin system resonances. These cross-peaks are observed even though the experiment was optimized to detect the small couplings between nitrogens and nonexchangeable protons on the imidazole ring. Resonances B and D belong to the same spin system with resonances 1 and 7. The pattern of cross-peaks indicates that these resonances all belong to the same positively charged histidine imidazole ring. Four other imidazole spin systems are correlated with resonances A, C, F, and H, respectively. The imidazole spin systems correlated with resonances F and H both display an HMQC cross-peak pattern characteristic of the Nδ1−H tautomer, while the imidazole spin system correlated with resonance A shows a cross-peak pattern characteristic of the Nϵ2−H tautomer. The imidazole spin system correlated with resonance C has an incomplete pattern, and the tautomeric form cannot be determined. Henceforth, imidazoles will be designated by the label of their associated exchangeable proton resonances, e.g., A, B/D, C. Two other imidazole spin systems remain uncorrelated to exchangeable proton resonances in the HMQC spectrum. The spin system containing nonexchangeable proton resonance 13 will later be correlated to peak G by one-dimensional NOEs (*vide infra*). Hence this imidazole will be designated G. Imidazole G has an incomplete cross-peak pattern in the HMQC spectrum, and its tautomeric form remains undetermined. The remaining spin system containing resonances 2 and 9 could not be correlated to an exchangeable proton resonance. This imidazole spin system and the undetected exchangeable proton resonance will be designated E. Imidazole E has a cross-peak pattern characteristic of the Nϵ2−H tautomer.

Two of the ^{15}N resonances in the expansion of the HMQC spectrum (Figure 2a) are not at their true ^{15}N chemical shift position because of folding of the spectrum in the ^{15}N dimension. This was verified both by acquiring a one-

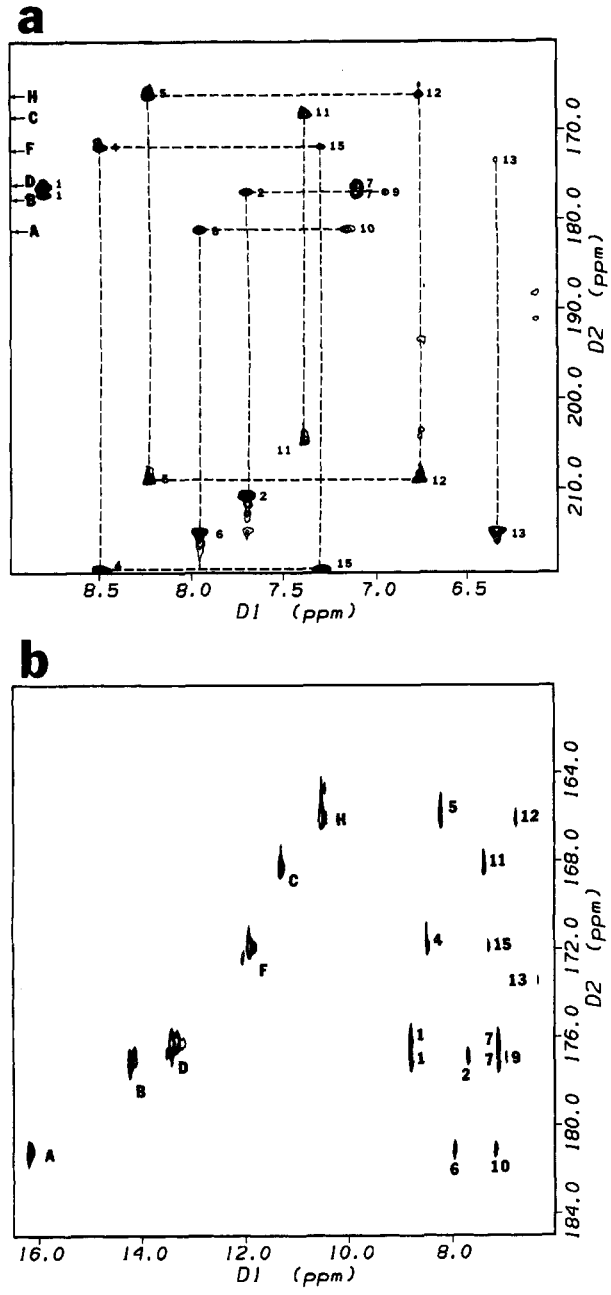

FIGURE 2: Expanded regions of a $^{15}N-^{1}H$ HMQC spectrum of uniformly ^{15}N-labeled *B. abortus* Cu–Zn SOD showing correlations between nitrogen and proton resonances on an imidazole ring. The spectra were recorded at 45 °C. Solution conditions were as described in the text. The HMQC experiment was set up to optimally detect 20 Hz *J* couplings. The residual H_2O resonance was suppressed by presaturation. (a) Region of the spectrum showing correlations of α, α+, and β nitrogen resonances to nonexchangeable proton resonances. Nitrogen resonances at *ca.* 205 and 209 ppm are folded from 234 and 230 ppm, respectively. There are two overlapping nitrogen resonances at *ca.* 215 ppm. (b) Region showing correlations of α and α+ nitrogen resonances to exchangeable and nonexchangeable proton resonances.

dimensional ^{15}N NMR spectrum and also by acquiring another HMQC spectrum with a different setting of the ^{15}N carrier frequency (data not shown). Thus, the lower of the cross-peaks labeled 11 at *ca.* 205 ppm actually resonates at 233.88 ppm, and cross-peaks labeled 5 and 12 at *ca.* 209 ppm actually resonate at 229.61 ppm. Additionally, two ^{15}N resonances from different imidazole spin systems overlap at 214.68 ppm. This was verified in the one-dimensional ^{15}N NMR spectrum (data not shown), which indicated that the resonance in question had double intensity.

Table 1: ^{1}H and ^{15}N Resonance Assignments of Histidine Imidazoles in the Active Site of *B. abortus* Cu–Zn Superoxide Dismutase[a]

residue	Nδ1–H	Nδ1	Cε1–H	Nε2–H	Nε2	Cδ2–H
His 45	13.44 (D)	176.21	8.81 (1)	14.25 (B)	177.17	7.12 (7)
His 48	Cu	233.88	7.39 (11)	11.32 (C)	168.23	7.69 (8)
His 50	11.94 (F)	171.89	8.50 (4)	Cu	218.88	7.32 (15)
His 73	Zn	214.68	6.35 (13)	11.92 (G)	173.46	6.54 (14)
His 82	Zn	214.68	7.97 (6)	16.20 (A)	181.16	7.16 (10)
His 90	Zn	210.52	7.69 (2)	n.o. (E)	176.88	6.95 (9)
His 128	10.53 (H)	166.09	8.23 (5)	Cu	229.61	6.79 (12)

[a] The numbers and letters in parentheses correspond to resonance labels indicated in the figures. All chemical shift values were determined from the $^{15}N-^{1}H$ HMQC spectrum measured at 45 °C except peaks 8 and 14, which were determined from the TOCSY spectrum measured at 45 °C, and peak G, which was determined from 21 °C one-dimensional difference NOE data. The symbols Cu and Zn indicate that the associated nitrogen is not protonated and is directly coordinated to the copper or zinc metal ions. The symbol n.o. indicates that the corresponding resonance was not observed.

All of the observed histidine β-type nitrogen resonances differed significantly from the characteristic chemical shift. Hydrogen bonding can cause nitrogen resonance shifts of up to 10 ppm from the characteristic value (Schuster & Roberts, 1979; Bachovkin, 1986), and changes in the tautomeric equilibrium may cause even larger shifts (Roberts *et al.*, 1982). All six of the observed β-type nitrogen resonances experienced upfield shifts in excess of the 10 ppm (Figure 2a). Shifts of this magnitude cannot be rationalized by hydrogen bonding interactions. In addition, these large shifts cannot be explained by altered tautomeric equilibria, because if that were the case, then the other nitrogen resonance within the same imidazole ring should be shifted a like amount in the opposite direction. The anomalous chemical shifts of the six β-type resonances occur because six histidine residues are ligands of either Cu or Zn metal ions in a subunit of Cu–Zn SOD. Thus, the β-type nitrogens of the histidine ligands would be coordinated to the metal ion via the lone pair of electrons on the nitrogen, and the electron distribution at the nitrogen atom would be significantly perturbed by this interaction. In particular, the π-electron density at the nitrogen atom might be expected to increase, resulting in a shift of the resonance to higher field (Witanowski *et al.*, 1972; Blomberg *et al.*, 1977). Metal ion binding apparently does not increase the π-electron density at the nitrogen as much as protonation of the nitrogen, so the observed shift is less than the observed 80 ppm shift on going from a β-type nitrogen to an α-type nitrogen. The anomalously shifted β-type nitrogen resonances therefore identify histidine residues that are metal ligands.

A two-dimensional homonuclear (^{1}H) TOCSY spectrum of *B. abortus* Cu–Zn SOD in H_2O was also acquired with a mixing time of 90 ms (data not shown). This spectrum showed correlations between the nonexchangeable proton resonances of an imidazole spin system and confirmed the correlations derived from the HMQC spectrum. Additionally, resonance 11 from imidazole C was correlated with resonance 8 (at 7.69 ppm), and resonance 13 from imidazole G was correlated with resonance 14 (at 6.54 ppm). The chemical shifts of the proton and nitrogen resonances of the seven identified histidine imidazoles are summarized in Table 1.

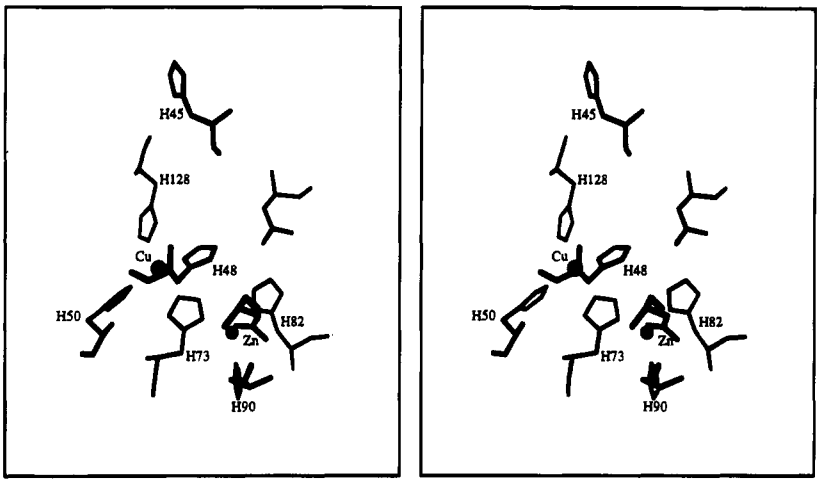

FIGURE 3: Stereo plot of a structural model of the active site of *B. abortus* Cu−Zn SOD showing several key conserved residues. The model was derived from the structure of the bovine enzyme (Tainer *et al.*, 1982; PDB: 2SOD), and the conserved residues have been renumbered to conform to the *B. abortus* sequence. The unlabeled aspartate residue in front of the Zn ion is D93.

Assignment of Histidine Imidazole NMR Resonances. Amino acid sequence alignment studies of prokaryotic and eukaryotic Cu−Zn SODs indicate the strong conservation of seven structurally and functionally important histidines near the active site (Getzoff *et al.*, 1989; Steinman & Ely, 1990; Beck *et al.*, 1990; Kroll *et al.*, 1991) and suggest that the active sites of the prokaryotic and eukaryotic enzymes have similar structures. Furthermore, the active site structures of the oxidized and reduced Cu−Zn SOD are expected to be very similar because the rate of catalysis is probably too fast for significant conformational rearrangements to occur (Paci *et al.*, 1990). This expectation is supported by NMR studies of the active site structure of the reduced eukaryotic enzymes (Cass *et al.*, 1977; Stoesz *et al.*, 1979; Paci *et al.*, 1990; Bertini *et al.*, 1991). Thus, it is reasonable to assume that the structure of the active site of reduced *B. abortus* Cu−Zn SOD is similar to those determined in X-ray crystallographic studies of the oxidized eukaryotic enzyme (Tainer *et al.*, 1982; Parge *et al.*, 1992). This assumption forms the basis for the sequence-specific assignment of the histidine imidazole resonances from the observation of a self-consistent pattern of intra- and inter-imidazole NOEs.

A model of the structure of the active site of reduced Cu−Zn SOD was derived from one subunit in the unit cell of the crystal structure of bovine Cu−Zn SOD (Tainer *et al.*, 1982) and is shown in Figure 3. The six histidine metal ligands and the one aspartate metal ligand are designated by their number in the aligned *B. abortus* Cu−Zn SOD amino acid sequence. His 48, His 50, and His 128 are Cu ligands, and His 73, His 82, and His 90 are Zn ligands. His 73 is the ligand that bridges both Cu and Zn in the oxidized form of the enzyme, but is bound only to Zn in the reduced form of the enzyme (McAdam *et al.*, 1977; Bailey *et al.*, 1980). There is possible ambiguity with the identification of His 82 as the Zn ligand because this residue is the C-terminal member of a His-His-His tract in the *B. abortus* Cu−Zn SOD sequence, and the actual metal ligand may be one of the other histidines in the tract. However, sequence alignment seems to favor His 82 (Beck *et al.*, 1990). A seventh histidine, His 45, is also conserved. In eukaryotic Cu−Zn SODs, this histidine is buried and near the active site and is hydrogen bonded to two backbone carbonyl oxygen atoms (Tainer *et al.*, 1982; Parge *et al.*, 1992). This residue has been shown to be positively charged even at high pH (Cass *et al.*, 1977; Stoesz *et al.*, 1979).

In order to predict NOEs, hydrogens were added using QUANTA software (Molecular Simulations), and the model was energy minimized using CHARMM (Molecular Simulations). On the basis of this structural model, one can predict NOEs between protons within a given imidazole and between protons on different imidazoles in the active site of *B. abortus* Cu−Zn SOD. The predicted NOEs are summarized in Table 2.

Even without resorting to NOE data, however, one can already make some preliminary assignments from the HMQC spectrum. Imidazole B/D has been shown to be fully protonated at pH 6.4, and its nitrogen-bound protons are protected from exchange with solvent. The imidazole ring of His 45 is the most likely one to have these properties, based on the structural model. Therefore, imidazole B/D and its associated resonances may be assigned to His 45. From the HMQC spectrum, imidazoles F and H have been shown to be metal ligands in the Nδ1−H tautomeric form. Therefore, they may be associated with His 50 and His 128, which are the only histidine metal ligands in that tautomeric form predicted by the structural model, although which corresponds to His 50 and which to His 128 remains to be determined. Imidazoles A, C, E, and G have been shown to be the remaining metal ligands, and all are in the Nϵ2−H tautomeric form.

An expanded region of the two-dimensional NOESY spectrum of *B. abortus* Cu−Zn SOD is shown in Figure 4a. The expansion shows NOE cross-peaks between exchangeable and nonexchangeable imidazole proton resonances. The NOESY spectrum confirms the correlation of resonances within an imidazole spin system and the tautomeric form of the imidazole ring. Thus, peaks F and H show only one intra-imidazole cross-peak each, to peaks 4 and 5, respectively. This agrees with the HMQC data which indicate that imidazole F and imidazole H are Nδ1−H tautomers. Similarly, imidazole A is confirmed as an Nϵ2−H tautomer because of the presence of two intra-imidazole cross-peaks, 6 and 10. Imidazole C is now shown to be in the Nϵ2−H tautomeric form by the presence of two intra-imidazole cross-peaks, 8 and 11. Imidazole B/D is confirmed as being positively charged, with peak B corresponding to the Nϵ2

Table 2: Predicted and Observed Nuclear Overhauser Effects in the Active Site of *B. abortus* Cu−Zn Superoxide Dismutase

NOE partners[a]		NOE intensity	
		predicted[b]	obsd[c]
H50 Nδ1−H (F)	H50 Cε1−H (4)	s	s
H128 Nδ1−H (H)	H128 Cε1−H (5)	s	s
H82 Nε2−H (A)	H82 Cε1−H (6)	s	s
H82 Nε2−H (A)	H82 Cδ2−H (10)	s	s
H48 Nε2−H (C)	H48 Cδ2−H (8)	s	s
H48 Nε2−H (C)	H48 Cε1−H (11)	s	s
H45 Nε2−H (B)	H45 Cε1−H (1)	s	s
H45 Nε2−H (B)	H45 Cδ2−H (7)	s	s
H45 Nδ1−H (D)	H45 Cε1−H (1)	s	s
H73 Nε2−H (G)	H73 Cε1−H (13)	s	s[d]
H73 Nε2−H (G)	N73 Cδ2−H (14)	s	s[d]
H90 Nε2−H (E)	H90 Cε1−H (2)	s	−
H90 Nε2−H (E)	H90 Cδ2−H (9)	s	−
H48 Nε2−H (C)	H73 Cε1−H (13)	w	m
H50 Nδ1−H (F)	H73 Cδ2−H (14)	v	v
H48 Nε2−H (C)	H128 Cδ2−H (12)	w	w
H48 Nε2−H (C)	H82 Cε1−H (6)	s	s
H48 Nε2−H (C)	H82 Nε2−H (A)	w	v[d]
H73 Nε2−H (G)	H48 Cε1−H (11)	w	m[d]
H73 Nε2−H (G)	H50 Cδ2−H (15)	w	m[d]
H73 Nε2−H (G)	H50 Cε1−H (4)	w	o[d]
H50 Cε1−H (4)	H128 Cε1−H (5)	s	o
H50 Cε1−H (4)	H73 Cδ2−H (14)	w	m
H73 Cδ2−H (14)	H50 Cδ2−H (15)	s	−
H48 Cε1−H (11)	H128 Cδ2−H (12)	s	s
H48 Cε1−H (11)	H73 Cε1−H (13)	m	w
H48 Cδ2−H (8)	H73 Cε1−H (13)	v	−
H82 Cε1−H (6)	H48 Cε1−H (11)	m	w
H82 Cε1−H (6)	H48 Cδ2−H (8)	w	o
H82 Cε1−H (6)	H73 Cε1−H (13)	s	s

[a] The numbers and letters in parentheses correspond to resonance labels indicated in the figures and in Table 1. [b] NOEs are predicted from interproton distances measured in the structural model shown in Figure 3. Intensities were classified: strong (≤2.7 Å), s; medium (2.7−3.3 Å), m; weak (3.3−4.1 Å), w; and very weak (4.1−4.9 Å), v. [c] NOE intensities were classified semiquantitatively by comparison to intra-imidazole NOEs expected to be strong: strong, s; medium, m; weak, w; very weak, v.; not observed, −; and overlapped (intensity undetermined), o. [d] Data from one-dimensional spectra.

proton and peak 1 corresponding to the Cε1 proton. No cross-peaks are observed from exchangeable resonances of imidazole G or E because these resonances are broadened excessively by solvent exchange at the temperature at which the NOESY spectrum was acquired, 45 °C.

The observation of a cross-peak from peak 4 (belonging to imidazole F) to resonance H indicates that imidazole H must belong to His 128 and imidazole F is part of His 50. The cross-peak corresponds to an NOE between the Cε1 proton of His 50 and the Nδ1 proton of His 128, which is the only NOE of this type (nonexchangeable proton to exchangeable proton) between histidines in the Nδ1−H tautomeric form that is predicted from the structural model. From peak F there is a cross-peak to peak 14, which belongs to imidazole G. The only predicted inter-imidazole NOE from the Nδ1 proton of His 50 (peak F) is to the Cδ2 proton of His 73. Thus, imidazole G is part of His 73. The structural model predicts NOEs from the Nε2 proton of His 48 to protons on three different histidine imidazoles: the Cδ2 proton of His 128 (imidazole H), the Cε1 proton of His 73 (imidazole G), and the Cε1 proton of His 82. There are NOE cross-peaks from peak C to peak 12 (Cδ2−H of His 128), to peak 13 (Cε1−H of His 73), and to peak 6 (Cε1−H of imidazole A). Thus, imidazole C must belong to His 48, and imidazole A is part of His 82. Imidazole E

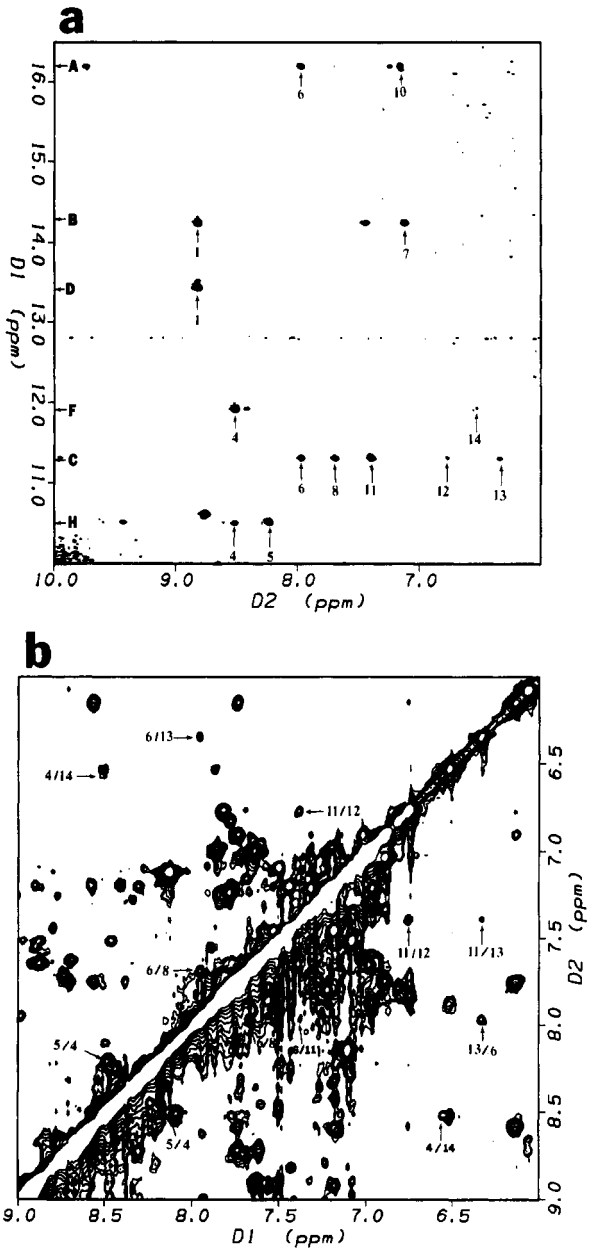

FIGURE 4: Expanded regions of the NOESY spectrum of *B. abortus* Cu−Zn SOD showing NOEs between imidazole protons. The spectra were recorded at 45 °C. Solution conditions and data acquisition parameters are described in the text. The H_2O resonance was suppressed by presaturation. (a) Region of the spectrum showing NOE cross-peaks between exchangeable and nonexchangeable proton resonances. (b) Region showing NOE cross-peaks between nonexchangeable proton resonances.

is assigned to His 90 by elimination. No inter-imidazole NOEs are expected from His 90, and none are observed from imidazole E.

A different expansion of the NOESY spectrum of *B. abortus* Cu−Zn SOD is shown in Figure 4b. This region of the spectrum shows NOE cross-peaks between nonexchangeable proton resonances on different imidazole rings. The observed NOEs are consistent with the assignments discussed above and the predictions of the structural model. Only two predicted NOEs between nonexchangeable imidazole protons were not observed: that between Cδ2−H of His 128 (peak 15) and Cδ2−H of His 73 (peak 14), and that between Cε1−H of His 73 (peak 13) and Cδ2−H of His 48 (peak 8).

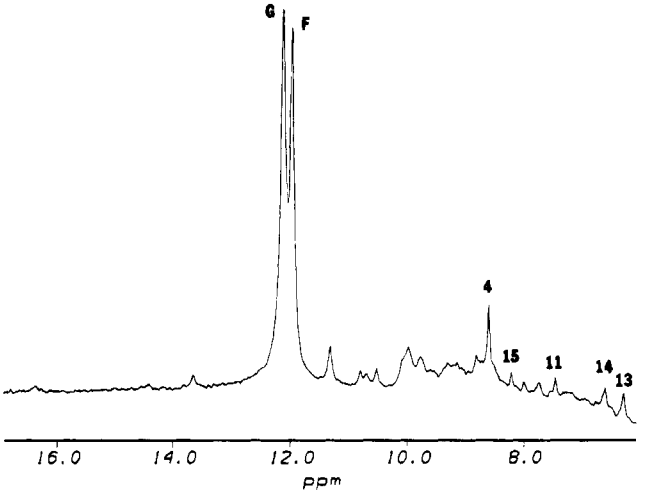

FIGURE 5: Downfield region of a one-dimensional difference NOE spectrum of *B. abortus* Cu−Zn SOD. The spectrum was recorded at 6 °C. Solution conditions and details of data acquisition are described in the text. The spectrum shows NOEs from peak G to peaks 15, 11, 14, and 13. The apparent NOE to peak 4 may be due to power spillover to peak F.

Additional NOE data were obtained using a one-dimensional difference NOE approach and suppression of the H_2O resonance by selective excitation with a jump-return pulse. These data were obtained at 6 °C, which resulted in a sharpening of peak G. There were some problems with power spillover and with poor cancellation of peaks when selectively saturating resonances upfield of 12 ppm. Nevertheless, with the aid of several control experiments to monitor power spillover and by repeating the experiment several times, NOEs from peak G to peaks 11, 13, 14, and 15 could be confirmed (Figure 5). The apparent strong NOE to peak 4 may be due in part to power spillover to peak F. An NOE from peak A to peak C was also confirmed (data not shown), although this NOE was also visible in the NOESY spectrum at lower contour levels. All other NOEs seen in Figure 4a were confirmed by one-dimensional difference NOE methods (data not shown). All predicted and observed NOEs are summarized in Table 2. The resonance assignments are summarized in Table 1.

DISCUSSION

In this work, we were able to assign all nonexchangeable proton resonances and all but one of the exchangeable proton resonances of the seven histidines in the active site of *B. abortus* Cu−Zn SOD (Table 1). The one unassigned proton resonance (exchangeable proton resonance of His 90) was not observed in any of the NMR spectra, presumably because of broadening of the resonance by exchange of the proton with solvent. In addition, all 14 ^{15}N resonances arising from active site histidines could be assigned in the $^{15}N-^{1}H$ HMQC spectrum of the uniformly ^{15}N-labeled enzyme (Table 1).

Comparison to Oxidized Eukaryotic Cu−Zn SOD. In assigning the imidazole proton resonances, we observed a self-consistent set of inter- and intra-imidazole NOEs, and there was excellent agreement between the observed NOEs and the NOEs predicted from the structural model (Table 2). All but four of the predicted NOEs were observed. For two of those, the absence of an NOE could be attributed to the broadening of exchangeable proton resonance of imidazole E (His 90) by solvent exchange. A third unobserved NOE, between peak 8 (His 48 Cδ2−H) and peak 13 (His 73 Cε1−H), is predicted to be very weak and may very well be beyond the limit of detection of the NOE method. The magnitudes of the observed and predicted NOEs agree semiquantitatively (Table 2). Moreover, the tautomeric states of the imidazoles and the identity of imidazole proton resonances deduced from the HMQC spectrum (independent of any structural assumptions) are also consistent with the assignments and the predictions of the structural model based on the X-ray crystal structure of oxidized eukaryotic Cu−Zn SOD. It is unlikely that the active site structure of the prokaryotic enzyme could be significantly different from that of the eukaryotic Cu−Zn SOD and still give rise to NMR spectra that could be assigned in a manner to give such excellent agreement between observed and predicted NMR parameters. Thus, our assumption that the structure of the active site of reduced *B. abortus* Cu−Zn SOD is similar to that found in oxidized eukaryotic Cu−Zn SODs (Tainer *et al.*, 1982; Parge *et al.*, 1993) is validated.

This conclusion is strengthened if proton resonance assignments can be obtained independent of structural assumptions. We have been pursuing the sequential assignment of the ^{1}H NMR spectrum of reduced *B. abortus* Cu−Zn SOD using three-dimensional NMR methods (Kintanar & Chen, 1993). We have confirmed the assignment of His 45, His 48, His 50, and His 128 by these methods (Chen and Kintanar, unpublished results).

It is tempting to interpret differences between predicted and observed NOEs in terms of structural differences of the active sites of the oxidized eukaryotic enzyme and the reduced prokaryotic enzyme. One should do so with caution, however, because other factors can affect the magnitude of the observed NOEs (e.g., dynamics). Nevertheless, one predicted NOE differed substantially in the observed spectra, between peaks 15 (His 50 Cδ2−H) and 14 (His 73 Cδ2−H). No NOE was observed, instead of a predicted strong NOE. This difference is consistent with a structural relaxation of the remaining ligands of the Cu ion after its reduction and the release of His 73. The structural rearrangement must be rather subtle, however, because the magnitudes of other NOEs from protons of His 73 to protons of His 48 or His 50 do not differ substantially from predicted values.

Comparison to Reduced Eukaryotic Cu−Zn SODs. It is also worthwhile to compare our results to some of the previous ^{1}H NMR studies of reduced eukaryotic Cu−Zn SODs (Stoesz *et al.*, 1979; Burger *et al.*, 1980; Bertini *et al.*, 1991). The pattern of NOEs we observed for reduced *B. abortus* Cu−Zn SOD was in excellent agreement with the observations of Bertini *et al.* (1991) on the reduced human enzyme, indicating that the active site structures of prokaryotic and eukaryotic enzymes in the reduced form are grossly similar. Any differences in the magnitudes of the observed NOEs were too small to allow meaningful inferences about detailed structural differences.

The chemical shift of exchangeable proton resonances may provide some insight into structural differences between the eukaryotic and prokaryotic enzymes. Resonances A, B, C, and D have been reliably assigned in a number of eukaryotic Cu−Zn SODs (Stoesz *et al.*, 1979; Burger *et al.*, 1980; Bertini *et al.*, 1991). In all eukaryotic Cu−Zn SODs, peak C has been observed between peaks B and D at roughly 13.3 ppm. In *B. abortus* Cu−Zn SOD, peak C (His 48 Nε2−H) is shifted upfield to 11.32 ppm, indicating that the environ-

ment of His 48 is significantly different than that of the analogous histidine in the eukaryotic enzymes. There are smaller chemical shift differences for some of the other exchangeable proton resonances (Bertini *et al.*, 1991), which may also reflect differences in the environments of the associated imidazoles, but only peak C shifts more than 0.6 ppm.

We may also compare the chemical shifts of assigned nonexchangeable proton resonances. The work of Bertini *et al.* (1991) on the human enzyme contains the most complete assignments. Only peaks 2 (His 90 Cϵ1−H), 8 (His 48 Cδ2−H), 11 (His 48 Cϵ1−H), and 14 (His 73 Cδ2−H) show chemical shift differences greater than 0.3 ppm, indicating possible differences in the environment of His 90, His 48, and His 73.

Finally, it is interesting to note that resonances E and G seem to be much more susceptible to broadening by solvent exchange in *B. abortus* Cu−Zn SOD than in the human enzyme. This indicates that the corresponding protons (His 90 Nϵ2−H and His 73 Nϵ2−H), in the *B. abortus* enzyme are more exposed to solvent.

These observations of altered environments of the histidines in the active site of *B. abortus* compared to the active site of the eukaryotic enzyme (Bertini *et al.*, 1991) are consistent with amino acid sequence alignments of the *B. abortus* sequence with eukaryotic sequences (Beck *et al.*, 1990), which indicate that major insertions and deletions occur in the loop regions that make up the active site. The structure of the loop regions in the *B. abortus* enzyme must differ from that in the eukaryotic enzyme, which is reflected in the altered environments of some active site histidine imidazoles.

Concluding Remarks. The results presented here offer strong evidence that the active site of a Cu−Zn SOD from a prokaryote has a similar structure as the active site of Cu−Zn SODs from eukaryotic species. Nevertheless, there appear to be real differences in the environments of His 48, His 73, and His 90 in the *B. abortus* enzyme compared to the human enzyme. Additionally, this work reiterates the advantage of using ^{15}N-labeling and ^{15}N−^{1}H HMQC methods to assign the proton and nitrogen resonances and to determine the tautomeric form of histidine imidazoles (van Dijk *et al.*, 1992; Pelton *et al.*, 1993). The results also show the unique ^{15}N chemical shifts of histidine imidazole nitrogens coordinated to metal ions. We are pursuing sequential assignments of the NMR spectra of *B. abortus* Cu−Zn SOD using three-dimensional heteronuclear NMR methods as a first step toward determining the high resolution solution structure of a prokaryotic Cu−Zn SOD. We have recently shown in our laboratory that Cu−Zn SOD from *B. abortus* is monomeric in solution (Cao, Tabatabai, and Kintanar, unpublished results). In the light of this finding, it is even more interesting that *B. abortus* Cu−Zn SOD has a similar level of activity and active site conformation as eukaryotic enzyme, because it is generally believed that subunit interactions are important for the catalytic activity of Cu−Zn SOD (Malinowski & Fridovich, 1979).

ACKNOWLEDGMENT

This research benefitted from the use of the 500 MHz NMR, Macromolecular Modelling, and Nucleic Acids Biotechnology Instrumentation Facilities at Iowa State University. We thank Dr. Mercedes Silva for her help in adding hydrogens to the model structure of reduced Cu−Zn SOD.

REFERENCES

Bachovkin, W. W. (1986) *Biochemistry 25*, 7751−7759.
Bachovkin, W. W., & Roberts, J. D. (1978) *J. Am. Chem. Soc. 100*, 8041−8047.
Bailey, D. B., Ellis, P. D., & Fee, J. A. (1980) *Biochemistry 19*, 591−596.
Bannister, J. V., Bannister, W. H., & Rotilio, G. (1987) *CRC Crit. Rev. Biochem. 22*, 111−180.
Bax, A., Griffey, R. H., & Hawkins, B. L. (1983) *J. Magn. Reson. 55*, 301−315.
Beck, B. L., Tabatabai, L. B., & Mayfield, J. E. (1990) *Biochemistry 29*, 372−376.
Beem, K. M., Rich, W. E., & Rajagopalan, K. V. (1974) *J. Biol. Chem. 249*, 7298−7305.
Bertini, I., Capozzi, F., Luchinat, C., Piccioli, M., & Viezzoli, M. S. (1991) *Eur. J. Biochem. 197*, 691−697.
Blomberg, F., Maurer, W., & Rüterjans, H. (1977) *J. Am. Chem. Soc. 99*, 8149−8159.
Bricker, B. J., Tabatabai, L. B., Judge, B. A., Deyoe, B. L., & Mayfield, J. E. (1990) *Infect. Immun. 58*, 2935−2939.
Burger, A. R., Lippard, S. J., Pantoliano, M. W., & Valentine, J. S. (1980) *Biochemistry 19*, 4139−4143.
Cass, A. E. G., Hill, H. A. O., Smith, B. E., Bannister, J. V., & Bannister, W. H. (1977) *Biochemistry 16*, 3061−3066.
Cass, A. E. G., Hill, H. A. O., Bannister, J. V., & Bannister, W. H. (1979) *Biochem. J. 177*, 477−486.
Drobny, G., Pines, A., Sinton, S., Weitekamp, D., & Wemmer, D. (1979) *Faraday Div. Chem. Soc. Symp. 13*, 49−55.
Fee, J. A., & Bull, C. (1986) *J. Biol. Chem. 261*, 13000−13005.
Forman, H. J., & Fridovich, I. (1973) *J. Biol. Chem. 248*, 2645−2649.
Fridovich, I. (1986) *Adv. Enzymol. 58*, 61−97.
Getzoff, E. D., Tainer, J. A., Stempien, M. M., Bell, G. I., & Hallewell, R. A. (1989) *Proteins: Struct., Funct., Genet. 5*, 322−336.
Harbison, G., Herzfeld, J., & Griffin, R. G. (1981) *J. Am. Chem. Soc. 103*, 4752−4754.
Hoffman, D. W., & Spicer, L. D. (1991) In *Techniques in Protein Chemistry II* (Villafranca, J. J., Ed.) pp 409−416, Academic Press, San Diego.
Jeener, J., Meier, B. H., Bachmann, P., & Ernst, R. R. (1979) *J. Chem. Phys. 71*, 4546−4553.
Kintanar, A., & Chen, Y.-L. (1993) *J. Cell. Biochem. 17C*, 277.
Kintanar, A., Metzler, C. M., Metzler, D. E., & Scott, R. D. (1991) *J. Biol. Chem. 266*, 17222−17229.
Klug, D., Rabani, J., & Fridovich, I. (1972) *J. Biol. Chem. 247*, 4839−4842.
Kroll, J. S., Langford, P. R., & Loynds, B. M. (1991) *J. Bacteriol. 173*, 7449−7457.
Laemmli, U. K. (1970) *Nature 227*, 680−685.
Levy, G. C., & Lichter, R. L. (1979) *Nitrogen-15 Nuclear Magnetic Resonance Spectroscopy*, John Wiley & Sons, New York.
Lippard, S. J., Burger, A. R., Ugurbil, K., Pantoliano, M. W., & Valentine, J. S. (1977) *Biochemistry 16*, 1136−1141.
Lowry, O. H., Rosebrough, N. J., Farr, A. L., & Randall, R. J. (1951) *J. Biol. Chem. 193*, 265−275.
Malinowski, D. P., & Fridovich, I. (1979) *Biochemistry 18*, 5055−5060.
Marion, D., & Wüthrich, K. (1983) *Biochem. Biophys. Res. Commun. 113*, 967−974.
Martin, J. P., & Fridovich, I. (1981) *J. Biol. Chem. 256*, 6080−6089.
McAdam, M. E., Fielden, E. M., Lavelle, F., Calabrese, L., Cocco, D., & Rotilio, G. (1977) *Biochem. J. 167*, 271−274.
McCord, J. M., & Fridovich, I. (1969) *J. Biol. Chem. 244*, 6080−6089.
Munowitz, M., Bachovkin, W. W., Herzfeld, J., Dobson, C. M., & Griffin, R. G. (1982) *J. Am. Chem. Soc. 104*, 1192−1196.
Paci, M., Desideri, A., Sette, M., Ciriolo, M. R., & Rotilio, G. (1990) *FEBS Lett. 263*, 127−130.
Parge, H. E., Hallewell, R. A., & Tainer, J. A. (1992) *Proc. Natl. Acad. Sci. U.S.A. 89*, 6109−6113.

Pelton, J. G., Torchia, D. A., Meadow, N. D., & Roseman, S. (1993) *Protein Sci. 2*, 543−558.
Plateau, P., & Guéron, M. (1982) *J. Am. Chem. Soc. 104*, 7310−7311.
Puget, K., & Michelson, A. M. (1974) *Biochem. Biophys. Res. Commun. 58*, 830−838.
Puget, K., Lavelle, F., & Michelson, A. M. (1977) in *Superoxide and Superoxide Dismutases* (Michelson, A. M., McCord, J. M., & Fridovich, I., Eds.) pp 139−150, Academic Press, London.
Redford, S. M., McRee, D. E., Getzoff, E. D., Steinman, H. M., & Tainer, J. A. (1990) *J. Mol. Biol. 212*, 449−451.
Roberts, J. D., Yu, C., Flanagan, C., & Birdseye, T. R. (1982) *J. Am. Chem. Soc. 104*, 3945−3949.
Robillard, G., & Shulman, R. G. (1974) *J. Mol. Biol. 86*, 519−540.
Roe, J. A., Butler, A., Scholler, D. M., Valentine, J. S., Marky, L., & Breslauer, K. J. (1988) *Biochemistry 27*, 950−958.
Rosenberg, A. H., Lade, B. N., Chui, D.-S., Lin, S.-W., Dunn, J. J., & Studier, F. W. (1987) *Gene 56*, 125−135.
Rotilio, G., Bray, R. C., & Fielden, E. M. (1972) *Biochim. Biophys. Acta 268*, 605−609.
Saiki, R. K., Gelfand, D. H., Stoffel, S., Scharf, S. J., Higuchi, R., Horn, G. T., Mullis, K. B., & Erlich, H. A. (1988) *Science 239*, 487−494.
Sambrook, J., Fritsch, E. F., & Maniatis, T. (1989) *Molecular Cloning: A Laboratory Manual, 2nd* ed., Cold Spring Harbor Laboratory Press, Cold Spring Harbor, NY.
Schuster, I. I., & Roberts, J. D. (1979) *J. Org. Chem. 44*, 3864−3867.
Shaka, A. J., Keeler, J., Frenkiel, T., & Freeman, R. (1983) *J. Magn. Reson. 52*, 335−338.
Sklenar, V., & Bax, A. (1987) *J. Magn. Reson. 74*, 469−479.
States, D. J., Haberkorn, R. A., & Ruben, D. J. (1982) *J. Magn. Reson. 48*, 286−292.
Steffens, G. J., Bannister, J. V., Bannister, W. H., Flohe, L., Gunzler, W. A., Kim, S.-M. A., & Otting, F. (1983) *Hoppe-Seyler's Z. Physiol. Chem. 364*, 675−690.
Steinman, H. M. (1982) *J. Biol. Chem. 257*, 10283−10291.
Steinman, H. M. (1985) *J. Bacteriol. 162*, 1255−1260.
Steinman, H. M. (1987) *J. Biol. Chem. 262*, 1882−1887.
Steinman, H. M., & Ely, B. (1990) *J. Bacteriol. 172*, 2901−2910.
Stoesz, J. D., Malinowski, D. P., & Redfield, A. G. (1979) *Biochemistry 18*, 4669−4675.
Studier, F. W., & Moffat, B. A. (1986) *J. Mol. Biol. 189*, 113−130.
Summers, M. F., Marzilli, L. G., & Bax, A. (1986) *J. Am. Chem. Soc. 108*, 4285−4294.
Tainer, J. A., Getzoff, E. D., Beem, K. M., Richardson, J. S., & Richardson, D. C. (1982) *J. Mol. Biol. 160*, 181−217.
Valentine, J. S., Pantoliano, M. W., McDonnell, P. J., Burger, A. R., & Lippard, S. J. (1979) *Proc. Natl. Acad. Sci. U.S.A. 76*, 4245−4249.
van Dijk, A. A., Scheek, R. M., Dijkstraa, K., Wolters, G. K., & Robillard, G. T. (1992) *Biochemistry 31*, 9063−9072.
Witanowski, M., Stefaniak, L., Januszewski, H., Grabowski, Z., & Webb, G. A. (1972) *Tetrahedron 28*, 637−653.
Wüthrich, K. (1986) *NMR of Proteins and Nucleic Acids*, John Wiley & Sons, New York.
Zubay, G. (1988) *Biochemistry, 2nd* ed., Macmillan, New York.

BI950646H